

Site-selective magnetic moment collapse in compressed Fe₅O₆*

Qiao-Ying Qin(秦巧英)^{1#}, Ai-Qin Yang(杨爱芹)^{1#}, Xiang-Ru Tao(陶相如)¹, Liu-Xiang Yang(杨留响)², Hui-Yang Gou(侯慧阳)^{2**}, and Peng Zhang(张朋)^{1**}

¹ MOE Key Laboratory for Nonequilibrium Synthesis and Modulation of Condensed Matter, School of Physics, Xi'an Jiaotong University, Xi'an, 710049, China

² Center for High Pressure Science and Technology Advanced Research, Beijing, 100094, China

*Supported by the National Natural Science Foundation of China under Grant No. 11604255, U1930401 and the Natural Science Basic Research Program of Shaanxi under Grant No. 2021JM-001.

The two authors contribute equally to this work.

**Corresponding author. Email: zpantz@xjtu.edu.cn (P. Zhang)
huiyang.gou@hpstar.ac.cn (H.Y. Gou)

Iron oxide is one of the most important components in Earth's mantle. Recent discovery of the stable presence of Fe₅O₆ at Earth's mantle environment stimulates significant interests in the understanding of this new category of iron oxides. In this paper, we report the electronic structure and magnetic properties of Fe₅O₆ calculated by the density functional theory plus dynamic mean field theory (DFT+DMFT) approach. Our calculations indicate that Fe₅O₆ is a conductor at the ambient pressure with dominant Fe-3*d* density of states at the Fermi level. The magnetic moments of iron atoms at three non-equivalent crystallographic sites in Fe₅O₆ collapse at significantly different rate under pressure. Such site-selective collapse of magnetic moments originates from the shifting of energy levels and the consequent charge transfer among the Fe-3*d* orbits when Fe₅O₆ is being compressed. Our simulations suggest that there could be high conductivity and volume contraction in Fe₅O₆ at high pressure, which may induce anomalous features in seismic velocity, energy exchange, and mass distribution at the deep interior of Earth.

PACS: 75.40.Mg; 91.60.Gf; 91.60.Pn

Iron oxide is one of the most abundant components in Earth's mantle, accounting for about 7.5% of the total mass of the Earth.^[1,2] In Earth's mantle the temperature ranges from 500 K to 3000 K and the pressure ranges from 20 GPa to 140 GPa. The behavior of iron oxide at high-temperature and high-pressure is essential for understanding the evolution of Earth's interior.^[3] At the ambient conditions, there are three known forms of iron oxides including wüstite (FeO), hematite (Fe₂O₃) and magnetite (Fe₃O₄).^[4] Iron oxides have also been widely used in industry,^[5-9] therefore attracted extensive interests in scientific communities.

Recently, a series of new iron oxides were identified at high pressure and high temperature including FeO₂,^[10,11] Fe₄O₅,^[12] Fe₅O₆,^[13] Fe₅O₇,^[14] Fe₇O₉^[14,15] and Fe₁₃O₁₉.^[16] Among these iron oxides Fe₅O₆ is synthesized by iron and hematite fine powder at ratio ($Fe + 2Fe_2O_3 = Fe_5O_6$) in a diamond anvil chamber at pressure ranges from 10 GPa to 20 GPa and temperature at about 2000 K.^[13] The experiment indicates that the crystal structure of Fe₅O₆ is orthorhombic (*Cmcm* space group) with lattice parameters of $a = 5.319579$ Bohr, $b = 18.510432$ Bohr, $c = 28.367432$ Bohr at 11.4 GPa.^[13] There are three non-equivalent iron atoms and four unequal oxygen atoms in Fe₅O₆. As shown in Fig. 1, the iron atom at site-4*c* (Fe1) and the surrounding six oxygen atoms form a triangular prism, in contrast the other two iron atoms at site-8*f*1 (Fe2) and site-8*f*2 (Fe3) with their surrounding six oxygen atoms form octahedra respectively. Since Fe₅O₆ is phase stable under high temperature and high pressure, it is expected to be an important candidate material in

the interior of Earth along with other iron oxides. Experiment by Hikosaka *et al.* shows that Fe_5O_6 will decompose into $\text{FeO} + \text{Fe}_4\text{O}_5$ below 10 GPa and will decompose into $2\text{FeO} + \text{Fe}_3\text{O}_4$ above 38 GPa.^[17] Recent experiment by Ovsyannikov *et al.* indicates the coexistence of the Verwey-type charge-ordering and the dimerization of iron atoms below 275 K,^[18] where they find such charge ordering can be tuned by the Fe-Fe distance of the octahedral chain in Fe_5O_6 . They further suggest that Fe_5O_6 could be used for memory devices or switches by controlling its charge ordering around the room temperature.

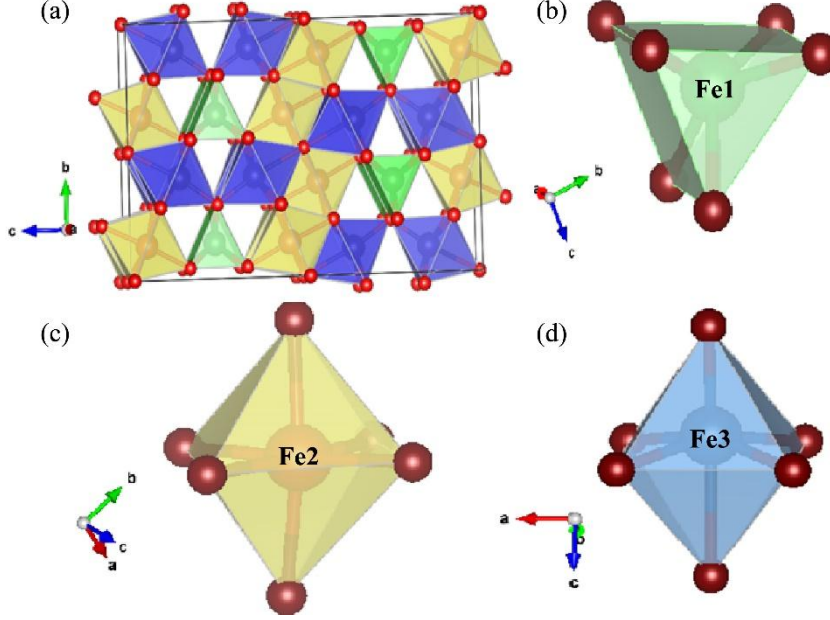


Fig. 1. (Color online) Crystal structure of Fe_5O_6 (a) the FeO_6 trigonal prism at site-4c (Fe1) in green color, (b) the FeO_6 octahedra at site-8f1 (Fe2) in yellow color and (c) the FeO_6 octahedra at site-8f2 (Fe3) in blue color.

The discovery of energetically stable Fe_5O_6 at high pressure opens up the possibility that it could be new candidate of Earth's mantle material. Unfortunately so far the experimental and the theoretical researches of Fe_5O_6 at the Earth's mantle conditions are very limited.^[13,17,18] In this paper, we use the DFT+DMFT^[19] method to calculate the electronic and the magnetic properties of paramagnetic Fe_5O_6 at high-pressure and high temperature. Our calculation proves that Fe_5O_6 is a metal with site-dependent magnetic moment collapse at high pressure. We further find that such site-dependent magnetic moment collapse originates from the energy level shifting and the consequent charge transfer among the five Fe-3d orbits in Fe_5O_6 .

In DFT+DMFT calculations, we adopt the Wien2k package^[20] in order to derive the charge density, the eigenvector and the eigenenergy of crystal in DFT level. The Wu-Cohen^[21] exchange-correlation potential with $20 \times 20 \times 4$ k-points is used. The exact double counting method^[22] and the hybrid expansion continuous-time quantum Monte Carlo (CTQMC) method^[23-25] are used for solving the self-consistent DMFT equation.^[26] In each DMFT iteration 10^7 Monte Carlo updates are used and the self-energy is derived from the Dyson's equation. The converged self-energy from DMFT is used to update the new charge density and the new Kohn-Sham potential for the next DFT calculation. The *DFT + DMFT* loops iterate until the fully convergence of the charge density, the self-energy and the hybridization functions *etc.* The maximum entropy method is used for analytic continuation of the self-energy from the imaginary frequency to the real frequency.^[27]

We employ the constrained density functional theory method^[28] to determine the screened Coulomb interaction U and the Hund's coupling J among the Fe-3d electrons. In orthorhombic Fe_5O_6 there are three non-equivalent iron atoms Fe1 (site-4c), Fe2 (site-8f1) and Fe3 (site-8f2). We derive the Coulomb U and the Hund's J at $V_0=743.41 \text{ bohr}^3/\text{Fe}_5\text{O}_6$ and at $V=698.34$

bohr³/Fe₅O₆ (at 11.4 GPa, also noted as $R = (1 - V/V_0)\% = 5.25\%$ representing the rate of volume compression). At $V_0=743.41$ bohr³/Fe₅O₆ (U, J) = (5.15 eV, 1.03 eV) at Fe1, (5.08 eV, 0.97 eV) at Fe2, and (4.62 eV, 0.97 eV) at Fe3. At 11.4 GPa, (U, J) = (5.04 eV, 0.83 eV) at Fe1, (5.02 eV, 0.87 eV) at Fe2, and (4.45 eV, 0.95 eV) at Fe3. Since the value of the Coulomb interaction U and the Hund's coupling J is not sensitive to the sites of iron atoms and the volume of Fe₅O₆ per unit cell, throughout our DFT+DMFT calculations we choose the average (U, J) = (5.88 eV, 0.88 eV). DFT+U volume optimization with ($U - J = 5.0$ eV) predicts $V_0=743.41$ bohr³/Fe₅O₆ is the volume at the ambient pressure. In DFT+DMFT we further try (U, J) = (5.88 eV, 1.0 eV), (10.0 eV, 1.0 eV) and (10.0 eV, 0.88 eV) at the ambient conditions and find all the conclusions in this paper stay valid being independent of the specific values of U and J as presented above.

It is known that at ambient conditions iron oxides like FeO and Fe₂O₃ are insulators while in contrast Fe₃O₄ is metal. There is debate about the electronic conductivity of FeO₂.^[29,30] Our DFT+DMFT calculations prove that Fe₅O₆ is a metal at the ambient pressure like Fe₃O₄. In Fig. 2, we present the total and the partial density of states (DOS) of Fe₅O₆. The total DOS of Fe₅O₆ have large quasi-particle peaks at the Fermi level in Fig. 2(a) at 743.41 bohr³/Fe₅O₆ corresponding to the ambient pressure and in Fig. 2(b) at 408.88 bohr³/Fe₅O₆ of 45% volume compression. This proves the metallic nature of Fe₅O₆ either at the ambient pressure or at high pressure. Also the height of quasi-particle peaks is relatively lower in Fig. 2(b) since the bandwidth of Fe₅O₆ is enlarged at high pressure. It is clearly shown in Fig. 2(c) and Fig. 2(d) that the total DOS of Fe₅O₆ at the Fermi level E_F is dominated by the Fe-3d bands, which suggests that the conductivity of Fe₅O₆ is mainly contributed by the Fe-3d electrons.

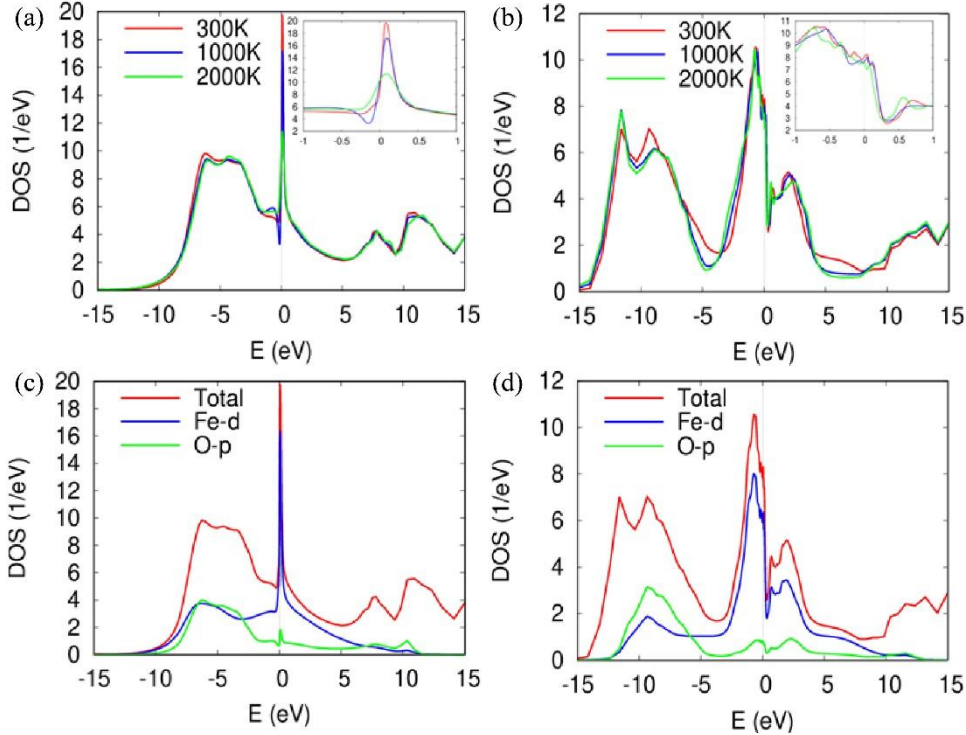


Fig. 2. The total density of states at 300 K, 1000 K, and 2000 K, (a) at the ambient pressure ($V_0=743.41$ bohr³/Fe₅O₆) and (b) at $R=45\%$ volume compression ($V=408.88$ bohr³/Fe₅O₆). The partial density of states of the Fe-3d orbits and the O-p orbits at 300 K (c) at the ambient pressure and (d) at 45% volume compression.

There will be collapse of magnetic moment in iron oxides at high pressure.^[30-36] Our DFT+DMFT calculations of the local magnetic moment $\sqrt{\langle m_z^2 \rangle}$ indicate that there is site-selective magnetic moment collapse in Fe₅O₆ under compression. As shown in Fig. 3, when Fe₅O₆ is compressed the local magnetic moment of Fe2 (8f1) decreases first, then the local

magnetic moment of Fe3 (8f2), and the local magnetic moment of Fe1 (4c) is the last one to decrease. At the 45% volume compression endpoint, the magnetic moments of Fe2 (8f1) and Fe3 (8f2) saturate at about $0.8 \mu_B/Fe$ and $1.1 \mu_B/Fe$ respectively, in contrast the magnetic moment of Fe1 (4c) ends at about $1.4 \mu_B/Fe$. The dependence of the local magnetic moment on temperature and volume compression is summarized in the three diagrams in Fig. 4. It is clear that the magnetic moments of the three non-equivalent iron atoms always decrease as being compressed at any temperature from 300 K to 2000 K. Either at low temperature or at high temperature, the magnetic moment of Fe atoms collapses first at 8f1 position, and then 8f2 position, the last is at 4c position. In Fig. 4(a), 4(b) and 4(c), the green region that represents the magnetic moment of intermediate size expands as the temperature is increased, which indicates that decrement of the magnetic moment is slower at high temperature.

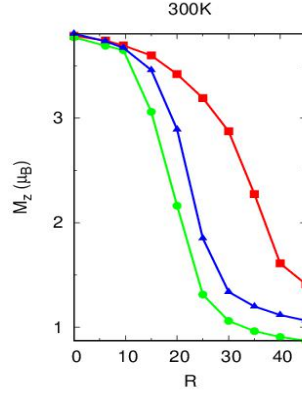


Fig. 3. The local magnetic moment of three non-equivalent iron atoms in Fe_5O_6 as a function of volume compression rate at 300 K. The red, the green, and the blue lines represent the local magnetic moments of Fe1 (site-4c), Fe2 (site-8f1), and Fe3 (site-8f2) respectively.

In transition metal oxides the collapse of magnetic moment is often accompanied by the insulator-metal transition and the collapse of volume.^[32-36] Thus the insulator-metal transition is presumed to be related to the collapse of magnetic moment. However in Fe_5O_6 we show the site-selective high spin-low spin transition of three iron atoms can be independent of the insulator-metal transition since Fe_5O_6 is always metallic from the ambient pressure to high pressure. Similar behavior has also been found in FeO_2 .^[30] It rises up the question that whether the metallization of Mott insulator is the consequence of the pressure driven high spin-low spin transition.

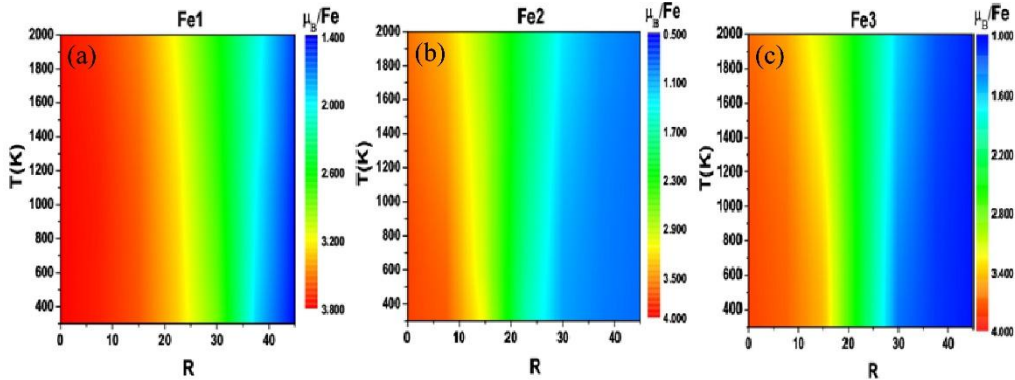


Fig.4. The dependence of local magnetic moments on temperature and volume compression rate at the three non-equivalent positions of Fe_5O_6 (a) Fe1 (site-4c), (b) Fe2 (site-8f1), and (c) Fe3 (site-8f2).

It has been proved that the magnetic moment collapse in transition metal oxides such as FeO and MnO originates from the transfer of electrons among the d -orbitals of the transition metals.^[32-34,36] As shown in Fig. 5, we present the Fe-3d electron occupancies at Fe1 (4c), Fe2 (8f1)

and Fe3 (8f2) of Fe₅O₆ at 300 K. When volume compression rate increases, at all three crystallographic non-equivalent sites the electron occupancies of the z^2 , $x^2 - y^2$ and xz orbitals increase, while the electron occupancies of the yz and xy orbitals decrease. It indicates the charge transfer from the yz and xy orbitals to the z^2 , $x^2 - y^2$ and xz orbitals upon the volume compression. However, for Fe1 (4c), the charge transfer from the yz and xy orbitals to the z^2 and xz orbitals start at relatively larger volume compression rate R than that of Fe2 (8f1) and Fe3 (8f2), and the electron occupancy of the $x^2 - y^2$ is almost constant until R is above 40%. This indicates that the electrons at Fe1 (4c) have stronger correlations than the electrons at Fe2 (8f1) and Fe3 (8f2). Such electron transfer among the Fe-3d orbitals is temperature dependent in that at higher temperature the charge will transfer at a lower rate.

The relationship between the local magnetic moment collapses of iron atoms and the charge transfer among the Fe-3d orbitals could be understood at the atomic limit. At the low pressure end all five Fe-3d orbitals have almost the same number of electrons and the magnetic moment is maximized at around $4.0 \mu_B/Fe$ due to the Hund's rule. At the high pressure limit when the yz and the xy orbitals lost all their electrons, then the six electrons on the z^2 , $x^2 - y^2$ and xz orbitals must form singlet pairs because of the Pauli's exclusion principle which leads to zero total magnetic moment.

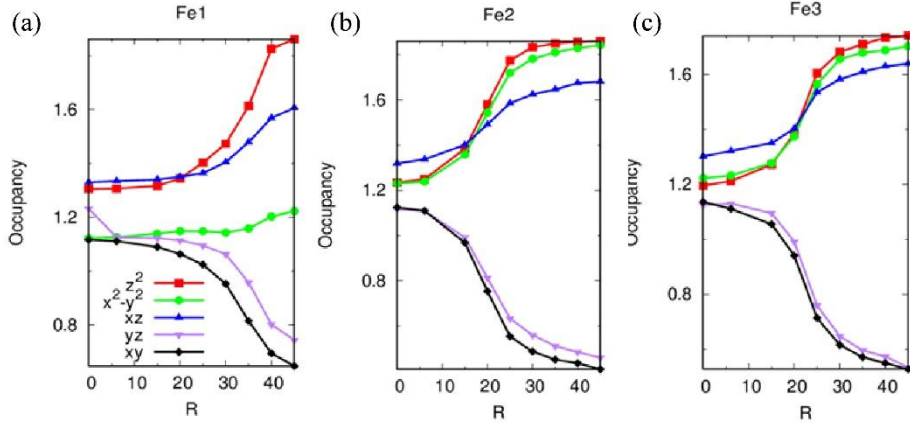


Fig.5. The electron occupancy number of the Fe-3d orbitals of atom (a) Fe1 (site-4c), (b) Fe2 (site-8f1) and (c) Fe3 (site-8f2) as a function of volume compression at 300 K.

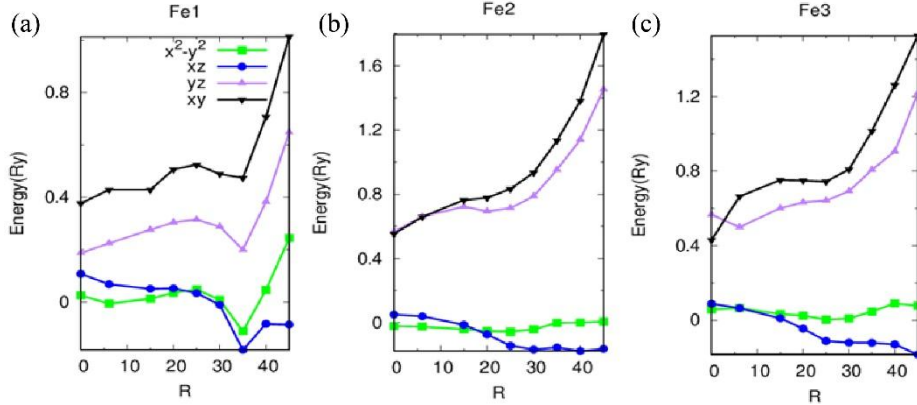


Fig.6. The energy differences of the Fe-3d orbitals of atom (a) Fe1 (site-4c), (b) Fe2 (site-8f1), and (c) Fe3 (site-8f2) as a function of volume compression rate at 300 K.

The transfer of electrons among the five Fe-3d orbitals originates from the shift of energy levels of the Fe-3d orbitals under compression. The energy difference of the $x^2 - y^2$, xz , yz and xy orbitals relative to the z^2 orbit under compression is shown in Fig. 6. In Fig. 6 (b) and Fig. 6 (c), upon compression energies of the yz and xy orbitals at Fe2 (8f1) and Fe3 (8f2) sites moves upward, however energies of the $x^2 - y^2$ orbitals stay almost invariant and energy of xz even decrease. Then naturally electrons on the yz and xy orbitals transfer to the z^2 , $x^2 - y^2$, and xz

orbitals in order to minimize the total energy in Fe₅O₆. In contrast in Fig. 6 (a) the orbital-energy differences of the *yz* and *xy* orbitals of Fe1 (4c) increase much slower under compression, which leads to the slower magnetic moment collapse as observed in Fig. 3.

In summary, we examine the electromagnetic properties of the recently discovered iron oxides Fe₅O₆ at the high pressure high temperature conditions of Earth's interior employing the DFT+DMFT method. Our calculations prove that the paramagnetic Fe₅O₆ is metallic either at the ambient pressure or at high pressure. The electronic conduction in Fe₅O₆ is dominated by the Fe-3*d* electrons. The local magnetic moments of three crystallographic non-equivalent iron atoms in Fe₅O₆ collapse at different rates as being compressed, which leads to site-dependent magnetic moment collapse. We further find that the site-dependent magnetic moment collapse in Fe₅O₆ originates from the energy level shifting and the consequent charge transfer among the five Fe-3*d* bands under volume compression. Since Fe₅O₆ is a candidate component of Earth's mantle beside the insulator FeO, the metallic nature of Fe₅O₆ suggests the conductivity of Earth's mantle could be higher than previously expected. The electronic conductivity and the related thermal conductivity of Earth's mantle may strongly affect the dynamics in Earth's deep interior. For example they could determine the energy exchange rate and the mass distribution of Earth's low mantle-core boundary, which may induce anomalous features in seismic velocity. Thus further investigations on Fe₅O₆ and other new iron oxides are called for the precise value of the electronic conductivity and the thermal conductivity at Earth's interior environment.

Acknowledgments. We thank the High Performance Computing platform of Xi'an Jiaotong University for providing the allocation of CPU time.

References

- [1] Crane R A and Scott T B [2013 *Journal of Nanotechnology* 10 1155](#)
- [2] Cornell R M and Schwertmann U 2004 *The Iron Oxides: Structure, Properties, Reactions, Occurrences and Uses*, 2nd ed. (New York: Wiley-VCH Verlag)
- [3] Wood B J, Bryndzia L T and Johnson K E [1990 *Science* 248 337](#)
- [4] Cornell R M and Schwertmann U 2004 *The Iron Oxides: Structure, Properties, Reactions, Occurrences and Uses*, 2nd ed. (New York: Wiley-VCH Verlag) p 1
- [5] Rosales S, Casillas N, Topete A, Cervantes O, Gonzalez G, Paz J A and Cano M E [2020 *Chin. Phys. B* 29 100502](#)
- [6] Li Zheng Hua, Li Xiang and Lu Wei [2019 *Chin. Phys. B* 28 077504](#)
- [7] Yu Wei-Qi, Qiu Yi-Chen, Xiao Hong-Jun, Yang Hai-Tao and Wang Ge-Ming [2019 *Chin. Phys. B* 28 108103](#)
- [8] Yan Wenjun, Zeng Xiaomin, Liu Huan, Guo Chunwei, Ling Min and Zhou Houpan [2019 *Chin. Phys. B* 28 106801](#)
- [9] Yang Yang, Zhang Qiang, Mi Wenbo and Zhang Xixiang [2020 *Chin. Phys. B* 29 083302](#)
- [10] Hu Q Y, Kim D Y, Yang W G, Yang L. X. and Meng Y [2016 *Nature* 534 241](#)
- [11] Nishi M, Kuwayama Y, Tsuchiya J and Tsuchiya T [2017 *Nature* 547 205](#)
- [12] Lavina B, Dera P, Kim E, Meng Y and Downs R T [2011 *Proc. Natl. Acad. Sci. USA* 108 17281](#)
- [13] Lavina B and Meng Y [2015 *Sci. Adv.* 1 e1400260](#)
- [14] Zhang X L, Niu Z W, Tang M, Zhao J Z and Cai L C [2017 *J. Alloys Compd.* 719 42](#)
- [15] Sinmyo R, Bykova E, Ovsyannikov S V, McCammon C and Kuppenko I [2016 *Sci. Rep.* 6 32852](#)
- [16] Merlini M, Hanfland M, Salamat A, Petitgirard S and Müller H [2015 *Am. Mineral.* 100 2001](#)

- [17] Hikosaka Koutaro, Sinmyo Ryosuke, Hirose Kei, Ishii Takayuki and Ohishi Yasuo [2019 *American Mineralogist* 104 1356](#)
- [18] Ovsyannikov S V, Bykov Maxim, Medvedev S A and Naumov P G [2020 *Angew. Chem.* 59 5632](#)
- [19] Kotliar G 2008 *Rev. Mod. Phys.* 78 865
- [20] Blaha P, Schwarz K, Madsen G K H, Kvasnick K and Luitz J [2001 in *Wien2K* \(ed. K. Schwarz\) \(Technische Universitat Wien\)](#)
- [21] Wu Z G and Cohen R E [2006 *Phys. Rev. B* 73 235116](#)
- [22] Haule K. [2015 *Phys. Rev. Lett.* 115, 196403](#)
- [23] Gull E., Millis A. J., Lichtenstein A. I., Rubtsov A. N., Troyer M. and Werner P. 2011 *Rev. Mod. Phys.* 83, 349
- [24] Werner P, Comanac A and de'Medici L [2006 *Phys. Rev. Lett.* 97 076405](#)
- [25] Haule K [2007 *Phys. Rev. B* 75 155113](#)
- [26] Georges A, Kotliar G, Krauth W and Rozenberg M J 1996 *Rev. Mod. Phys.* 68 13
- [27] Madsen G K H and Novak P 2005 *Europhys. Lett.* 69 777
- [28] Jarrell M. and Gubernatis J.E. 1996 *Physics Reports* 269 133
- [29] Bo G J, Kim D Y and Ji H S [2017 *Phys. Rev. B* 95 075144](#)
- [30] Koemets E [2021 *Phys. Rev. Lett.* 126 106001](#)
- [31] Cohen R E, Mazin I I and Isaak D G [1997 *Science* 275 654](#)
- [32] Greenberg Eran [2018 *Phys. Rev. X* 8 031059](#)
- [33] Kunes J, Korotin D M, Korotin M A, Anisimov V I and Werner P [2009 *Phys. Rev. Lett.* 102 146402](#)
- [34] Kunes J, Lukoyanov A V, Anisimov V I, Scalettar R T and Pickett W E [2008 *Nat. Mater.* 7 198](#)
- [35] Ohta K, Cohen R E, Hirose K, Haule K, Shimizu K and Ohishi Y [2012 *Phys. Rev. Lett.* 108, 026403](#)
- [36] Leonov I [2015 *Phys. Rev. B* 92 085142](#)